Characteristics of Turbulent Cross and Alongshore Momentum Exchanges During a Thermal Bar Episode in Lake Ontario

Messon B. Gbah

University of Michigan, Ann Arbor, MI 48108 U.S.A.

Raj C. Murthy

Nat. Water Res. Inst., Burlington, Ont. L7R 4A6, Canada.

Time series flow data obtained during the thermal bar episode of 17 April to 24 May 1990 in Lake Ontario are analyzed to provide a kinematic description of the coastal flow and cross-margin exchange characteristics. A thermal bar is a shore-parallel front which separates descending waters at or near the fresh water temperature of maximum density (4°C) during Spring and Fall seasons. Thermal bars are important because of their influence mixing, cross-shore exchanges, and the variability of biotic factors in coastal zones.

The analysis shows that cross-frontal exchange coefficients, K_y, are nearly constant and consistently smaller than along-frontal counterparts, K_x. Moreover, these exchange coefficients are several orders of magnitude smaller than typical coastal and oceanic values in the absence of the bar. The turbulent kinetic energy represents less than 6% of the total kinetic energy in the flow. These results suggest that small-scale horizontal fluctuations and cross-frontal turbulent momentum exchanges are severely inhibited in the spring during the thermal bar.

Introduction

The coastal zone of Lake Ontario supports large urban communities, industries, and power plants which depend on its basin for recreation, drinking water, and manufacturing. For this reason and other emerging environmental monitoring concerns such as pollution transport and waste dispersion in the coastal zone, there is a clear need to increase our understanding of nearshore dynamics through well-planed coastal transport experiments. Numerous such experiments conducted on the Great Lakes

(Blanton 1975; Blanton and Murthy 1974; Csanady 1972a; Csanady 1972b; Murthy and Dunbar 1981) have shown that strong meteorological events such as coastal fronts, episodes of strong winds, Kelvin waves, or thermal bars alter considerably the coastal flow regime.

A thermal bar is a mixing region which separates descending waters near the temperature of maximum density in most temperate large lakes in the Spring and Fall seasons. In the Spring, this mixing zone marks the transition from isothermal winter conditions to stratified summer conditions (Tikhomirov 1963; Rodgers 1966). The bar is often a well-defined shore-parallel front characterized by nearly vertical 4°C isotherms and convergent surface flows. The strength and persistence of the bar are a function of the surface fluxes and the local bathymetry (Gbah 1994). Thermal bars are important because of their inhibiting influence on turbulent mixing in the coastal zone and their effects on the spatio-temporal variability of biotic factors (LeFevre 1986, Franks 1992; Moll *et al.* 1993; Brandt 1993). Despite several studies, this inhibiting influence of the bar has yet to be fully understood or quantified.

In the present paper, we show the effects of the thermal bar on the flow regime and on turbulent cross-margin exchanges in Lake Ontario from April 17 to May 24, 1990. We begin this work with a description of the flow data after this introduction. Next, we characterize and establish the existence of the bar. In the fourth section, we present a theoretical framework for calculating the horizontal exchange coefficients. We conclude with the results and a summary in the last two sections.

The Data

The data consist of Eulerian time series of water temperature and currents (North and East components of velocity) obtained from an array of 6 SACM Brown current meters and Conductivity-Temperature-Depth (CTD) chain moored at a depth of 10 meters. Fig. 1 depicts the geographic location of the coastal chain off Port Darlington, Lake Ontario. The local bathymetry has a gentle slope with depths of 11 m at the innermost buoy, to 87.5 m at the outermost. The temperature and current meter data were of high quality, owing to periodic inspection and cleaning of the instrument array. The coastal chain was deployed perpendicular to the local bathymetry and extended 14.3 km offshore. This set up is designed to capture the onshore-offshore structure of the flow at fixed points along an axis perpendicular to the local shoreline. The available flow data time series spans April 10 to October 24, 1990 and the thermal bar episode was identified in mid-April to the end of May. The data sampling rate was 30 minutes, except at the second mooring from the shore in which the rate was 36 minutes. The coordinate system used is such that the x-axis is parallel to the shore and the y-axis is directed offshore along the instrument array. The time series data was first hourly averaged then, the North and East velocities were resolved into shore-parallel and shore-perpendicular components, u and v, respec-
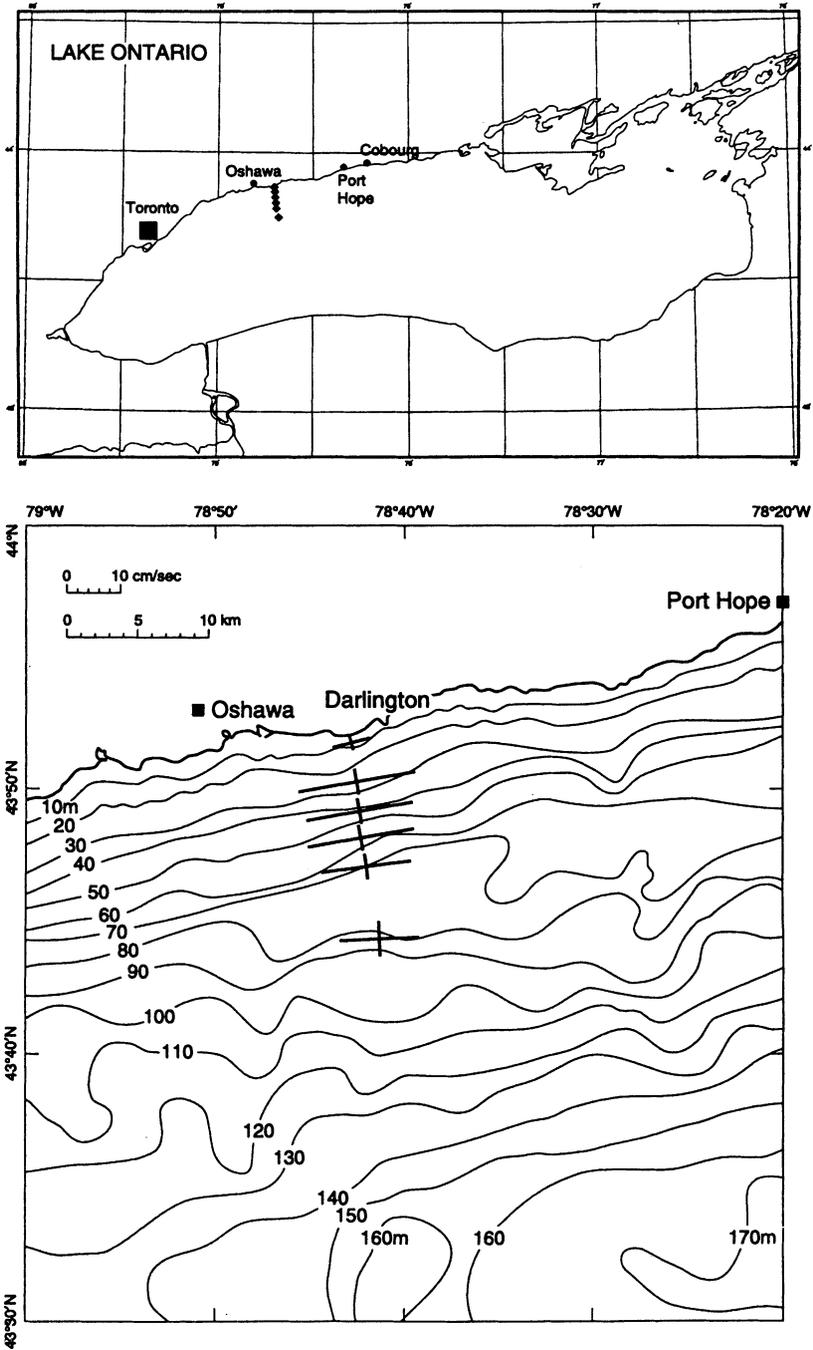
58

Fig. 1. Map of the coastal chain showing the coastal chain, local bathymetry, flow ellipses, and a nearly straight shoreline oriented 80 degrees from the North.

tively. A land-based tower at Toronto Island Airport provided hourly wind speeds and directions from April 1 to the end of November 1990.

Typical spectral kinetic energy plots of currents in the Great Lakes are characterized by a low frequency peak around 200 hours, a minimum around 30 hours, a dominant peak near 17 hours, and several smaller high frequency peaks and valleys associated with lake breeze (Murthy and Dunbar 1981). The low frequency spectral maximum (200 hours) corresponds to lake-wide synoptic wind forcing responsible for most of the energy in the flow. The 17-hour peak is the basin's response to inertial oscillations at the latitude of the Great Lakes. Murthy and Dunbar (1981) argue that the 30-hour spectral minimum is a characteristic feature of the energy transfer from large-scale basin wide circulation to the small-scale fluctuations in the flow. In the present work, we used an 18-to-24 hours low-pass Graham (1963) filter to separate the slowly varying mean flow from the high frequency fluctuating components which include free surface seiches, tidal, and inertial motions.

Description of the Thermal Bar

Longshore wind stresses are important to the nearshore flow because predominant wind events over Lake Ontario are generally in the East-West direction parallel to the local shoreline. Fig. 2 presents hourly longshore wind stresses and currents at all six stations. This figure shows that currents at all stations responded well to the East-West wind stresses. Winds and currents roses reveal that subsurface currents are essentially shore-parallel and that cross-shore velocities account for less than 5% of all subsurface currents intensities. Winds speeds were generally moderate and Rodgers (1966) has observed vernal thermal bars on Lake Ontario under similar wind conditions.

Fig. 3 shows satellite-derived surface temperature maps (SST) on April 16, May 2, May 8, and May 30. The 4°C isotherm indicates the position of the bar at the water surface. As heating continues, this isotherm migrates from the shores to deeper waters. These SST maps reveal average offshore migration bar speeds of 2, -1, and 9 cm/s between consecutive maps, starting with the April 16 map. Hence, these maps show that the thermal bar is dynamic and may move inshore during its overall offshore migration.

Fig. 4 illustrates weekly mean *in situ* temperatures at each mooring. The 4°C isotherm marks successive weekly mean positions of the bar at the instruments' depth of 10 metres. Fig. 4 also shows a large temperature gradient between the stations inward and outward of the bar. Rodgers (1966) and Tikhomirov (1968) first documented such temperature gradients typical of the thermal bar. An examination of the hourly *in situ* temperature time series from all six stations suggests that the thermal bar formed near the shore-most buoy on April 17 and reached the outermost buoy on May 24, 1990. Subsurface weekly offshore bar migration speeds obtained from
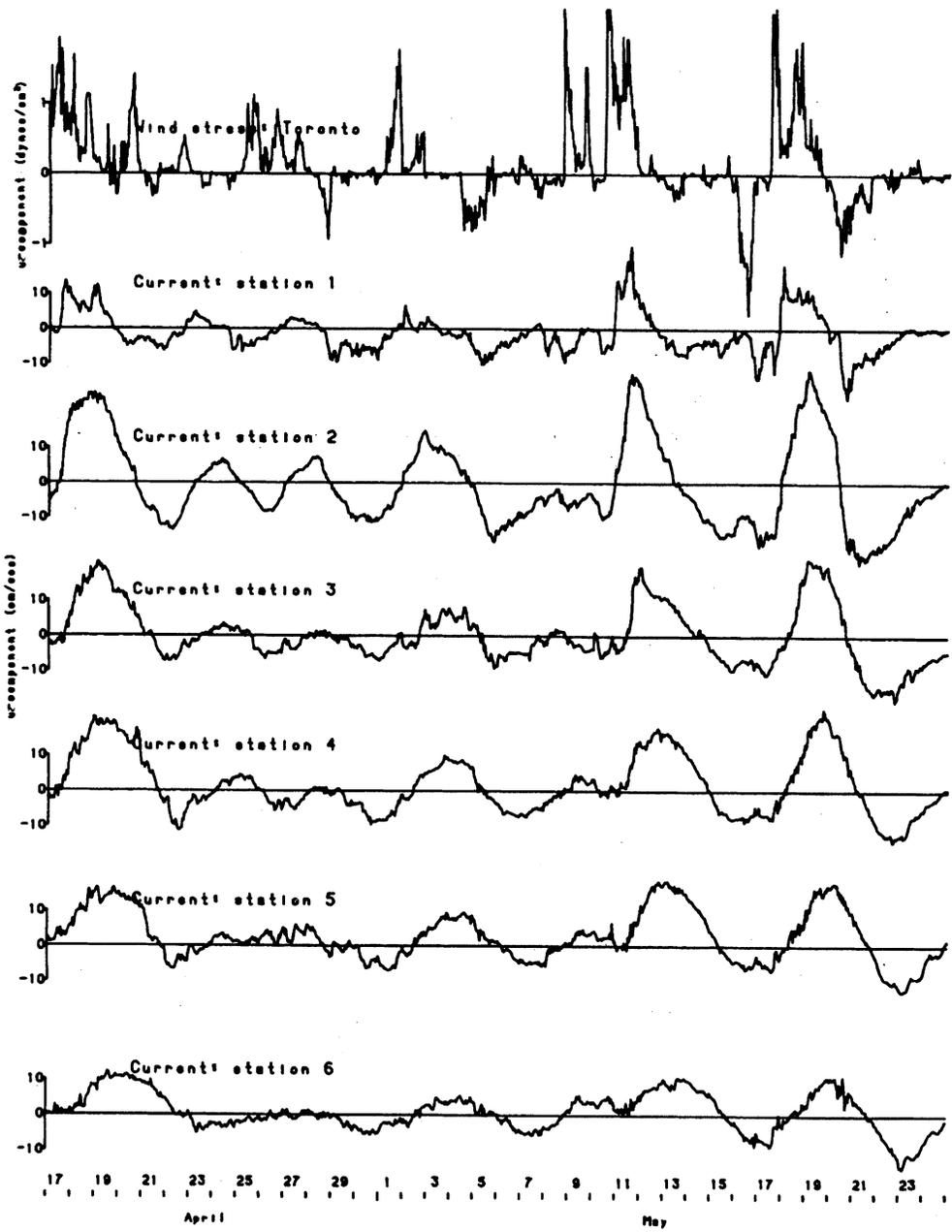
Fig. 2. Hourly averaged longshore wind stresses and currents at all moorings.

61

N

0 25 50 km

16 April 1990
Mean Temperature 3.1°C

02 May 1990
Mean Temperature 4.1°C

08 May 1990
Mean Temperature 4.0°C

30 May 1990
Mean Temperature 6.6°C
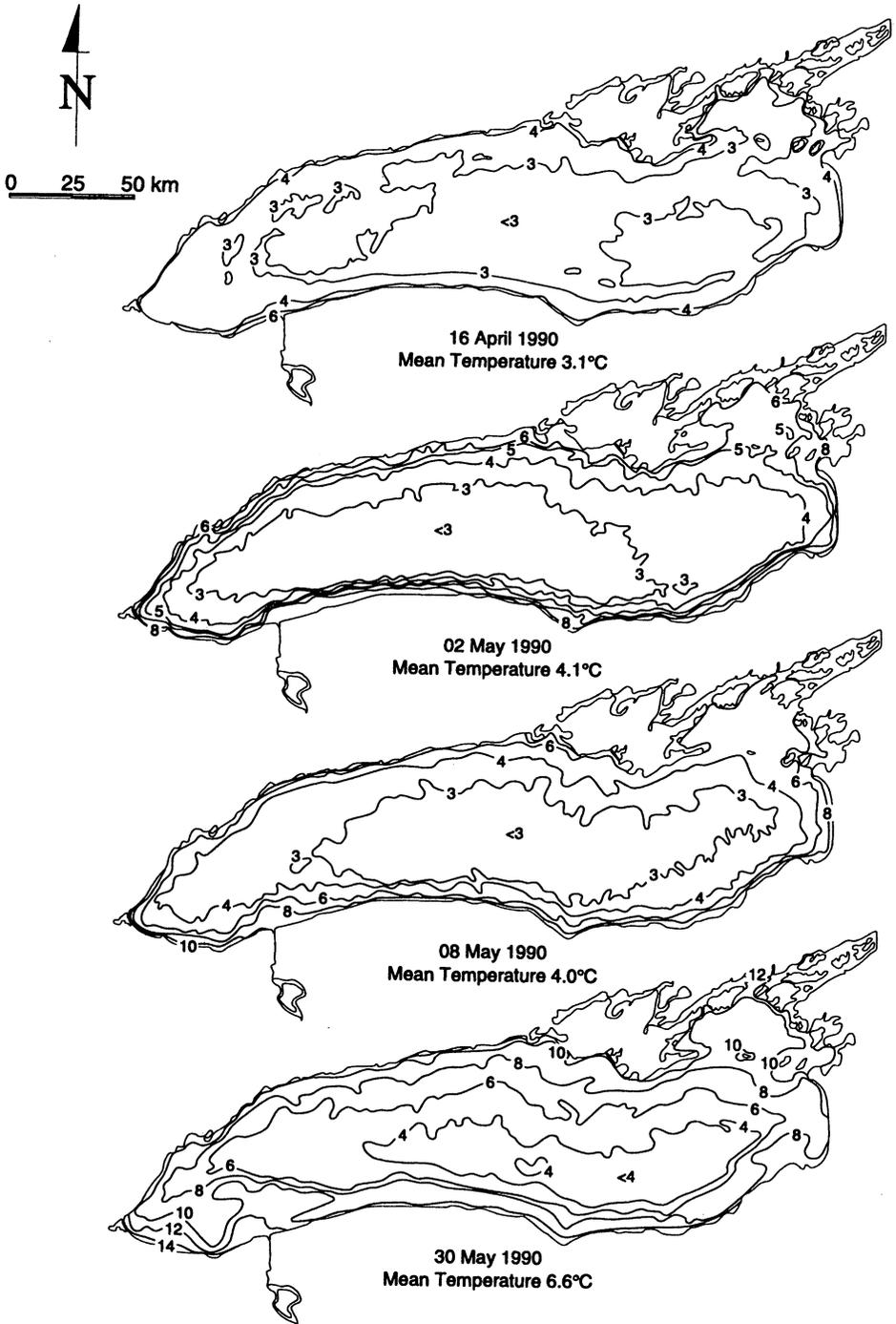
Fig. 3. Lake surface temperature (SST) maps showing successive positions of the thermal bar.

62

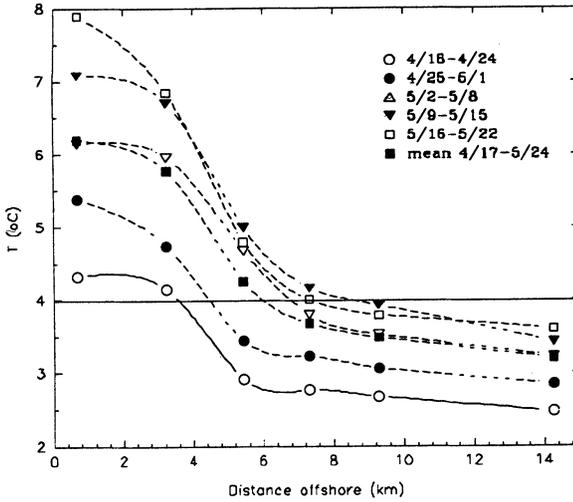Fig. 4. Weekly mean *in situ* temperatures as a function of the offshore distance from 4/17.
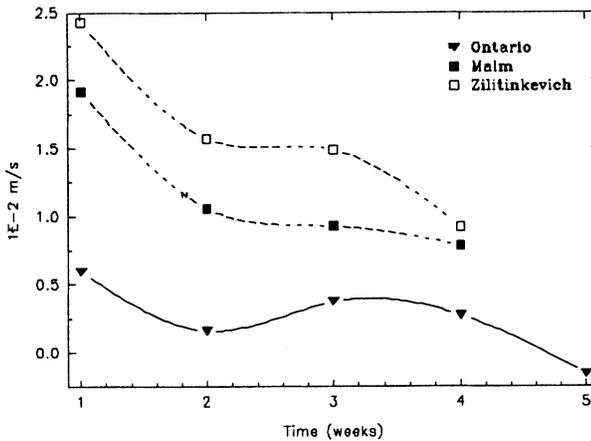
Fig. 5. Weekly bar migration speeds from: our data (▼), Malm *et al.* (1994) (■), predictions by Zilitinkevich *et al.* (1992) (□). Malm and Zilitinkevich's results are extracted from Fig. 11 of Malm *et al.* (1994). The zero on the time axis represents April 17, 1990 for our Lake Ontario data and May 15, 1992 for the other two curves.

these SST maps are presented Fig. 5, along with results by Malm *et al.* (1994) on Lake Ladoga and Zilitinkevich *et al.* (1992) therein. These weekly bar speeds are non-constant and clearly decrease over the heating season as shown in Fig. 5. That is, the bar slows down over time and eventually disappears. This decrease in speed with the offshore distance is explained by the fact that more heat is required to warm a deep offshore layer than is needed for a shallow one near the shore.

63

Theoretical Considerations

In order to parameterize the dispersal tendencies of the flow, we present a theoretical framework for relating Lagrangian current fluctuations to horizontal Eulerian (fixed point) turbulence exchange parameters. Let x denote the axis parallel to the shore, and y the axis positive outward along the instrument array. In a stationary and homogeneous field of turbulence with zero mean particle velocity, Taylor (1921) defines the Lagrangian exchange coefficient in terms of the variance of the Lagrangian particle displacement $x(t)$ at time t as

$$K_l = \frac{1}{2}\frac{\overline{dx^2}}{dt} = x\frac{\overline{dx}}{dt} = \int_0^t \overline{u_l'(\lambda)u_l'(\lambda)}\,d\lambda = \overline{u_l'^2}\int_0^t R_l(\tau)d\tau \qquad (1)$$

Here, $u_l'(t)$ denotes Lagrangian velocity fluctuations along the x-axis,

$$R_l(\tau) = \frac{\overline{u_l'(t)u_l'(t+\tau)}}{\overline{u_l'(t)u_l'(t)}}$$

is the Lagrangian autocorrelation function, and overbars denote time averaging.

The Lagrangian integrale time scale is defined by

$$\tau_l \equiv \int_0^\infty R_l(\tau)d\tau \qquad (2)$$

When the diffusion time has elapsed beyond some lag time t_l called the Lagrangian correlation time scale, the correlation function $R_l(\tau)$ will drop to zero. Physically t_l is the decay time scale of those eddies, which contribute significantly to the diffusion. Therefore, for large time scales $t > t_l$, the horizontal exchange coefficient attains a constant value $K_l = \overline{u_l'^2}\,\tau_l$.

Similarly, in the Eulerian frame of reference, we can obtain the Eulerian the velocity fluctuations $U_e'(\tau)$, the autocorrelation function $R_e(\tau)$, the Eulerian integrale time scale $\tau_e = \int_0^\infty R_e(\tau)d\tau$, and the Eulerian exchange coefficient $K_e = \overline{u_e'^2}\,\tau_e$.

Experimentally, it is difficult to measure Lagrangian current fluctuations and therefore the Lagrangian integral time scale. To calculate the horizontal exchange coefficients, we use the corresponding Eulerian values, which can be readily calculated from long time series of current measurements. Lumley and Danofsky (1964) have shown that, in a stationary and homogeneous field of turbulence, the Lagrangian variance $\overline{u_l'^2}$ can be assumed equivalent to the Eulerian variance $\overline{u_i'^2}$ for small scales. Hay and Pasquill (1959) have argued that the Lagrangian correlation function $R_l(\tau)$ and the Eulerian counterpart $R_e(\tau)$ have similar shape $R_e(\tau) = R_l(\beta\tau)$ where β is an empirical constant greater than unity. Introducing these assumptions, we rewrite the Eulerian exchange coefficient in terms of Eulerian statistics as

64

$$K_e \equiv \beta \, \overline{u_e'^2} \, \tau_e \tag{3}$$

While it is relatively easy to calculate $u_e'^2$ and τ_e from time series measurements of currents, the factor β is difficult to quantify, being a function of the energy spectra of current fluctuations, intensity of turbulence, and the stability of the water column. Hay and Pasquill (1959) and Haugen (1966) have reported values of β around 4, from atmospheric experiments. For oceanic cases, Schott and Quadfasel (1979) have determined values of β, a factor somewhat similar to , of 1.4 ± 0.4, based on simultaneous Lagrangian and Eulerian measurements in the Baltic. We have set $\beta \equiv 1$ as an average oceanic value in our calculations. This is a reasonable estimate of β since the goal of the present study is not the precise quantification of the numerical value the horizontal exchange coefficients.

As stated earlier, the above theoretical framework for calculating horizontal exchange coefficients is strictly valid in a field of stationary and homogeneous turbulence, which rarely exists in actual oceanic conditions. However, from the practical point of view, a climatology of the horizontal exchange characteristics can be established from a long time series of Eulerian currents, measured under actual oceanic conditions. The analysis presented in the paper is aimed towards this goal. For ease of notation, since all flow variables calculated are based on Eulerian measurements, we drop the subscript e for the rest of this work. Hence, K_x and K_y designate the alongshore and cross-shore component of K in an Eulerian frame of reference.

To complete the kinematic description of the subsurface coastal flow, we also present, in addition to the horizontal exchange coefficients (K_x, K_y), the mean currents (U, V) and temperature Θ: 1) The non-diagonal term $\overline{u'v'}$ (of the correlation tensor) which represents the Reynolds stresses per unit mass and measures the degree of anisotropy in the turbulence. 2) The total kinetic energy E, the kinetic energy e of the mean flow, and the turbulent kinetic energy q given by $(E, e, q) \equiv \frac{1}{2} (u^2 + v^2, \overline{u}^2 + \overline{v}^2, \overline{u'^2} + \overline{v'^2})$.

Cross-margin Exchanges Characteristics

Table 1 presents properties of the mean flow and horizontal turbulence characteristics during the thermal bar episode. The mean temperature decreases as one goes from the shore ,to deeper water. In addition, the velocity variances, and Reynolds stresses per unit mass remain small, suggesting that turbulent stresses and velocity fluctuations are suppressed during the spring when the thermal bar is present. The magnitude of the mean longshore currents, turbulent velocities, exchange coefficients, and velocity variances are all higher than the cross-shore counterparts, except the mean current at station 3. These results attest of the predominantly along-frontal nature of the flow.

Weekly mean currents (from April 17) during the thermal bar period are illustrat-

Table 1 – Characteristics of the flow during the vernal thermal bar.

| ID	1	2	3	4	5	6
Buoy Dist.(km)	0.68	3.24	5.42	7.30	9.28	14.27
U(cm/s)	-1.13	-0.70	0.09	1.64	2.77	0.92
V(cm/s)	-0.34	0.49	0.70	0.38	-0.08	0.15
θ(°C)	6.19	5.77	4.26	3.68	3.48	3.20
$\sqrt{u'^2}$(cm/s)	1.53	0.95	0.94	0.84	0.87	0.76
$\sqrt{v'^2}$(cm/s)	0.56	0.61	0.77	0.72	0.76	0.66
$u'v'$(cm^2/s^2)	-0.05	0.00	0.14	0.14	-0.03	-0.04
K_x(10^{4}cm^2/s)	1.297	0.355	0.347	0.278	0.317	0.181
K_y(10^{4}cm^2/s)	0.104	0.141	0.248	0.187	0.226	0.159
E(cm^2/s^2)	16.21	72.52	35.15	36.33	29.34	16.32
e(cm^2/s^2)	14.77	71.76	34.32	35.66	28.61	15.79
q(cm^2/s^2)	1.44	0.76	0.83	0.67	0.73	0.53
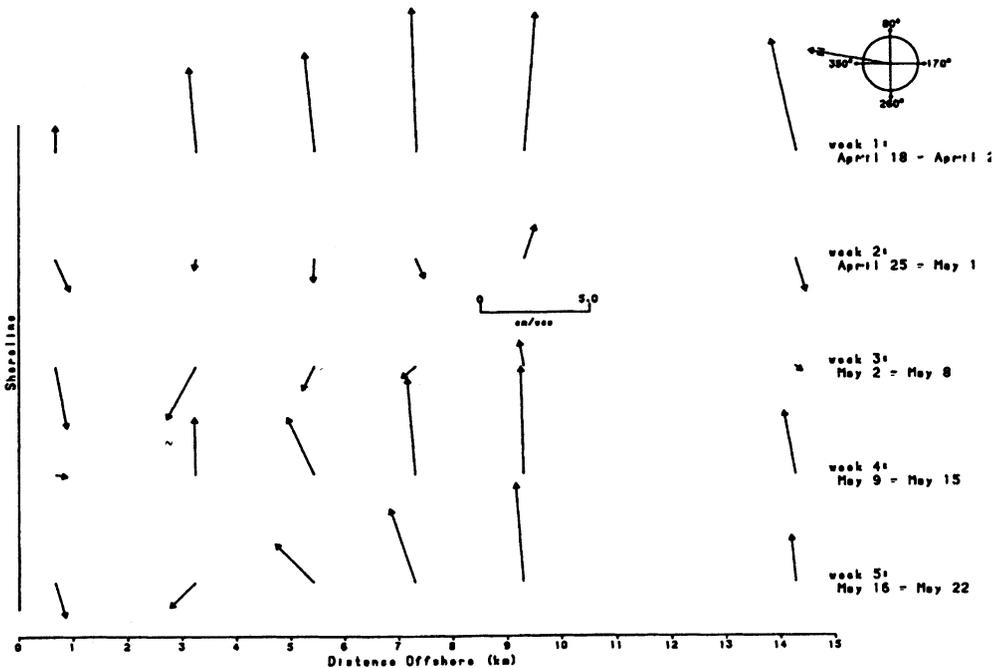
Fig. 6. Weekly mean flow current vectors at each mooring. The shoreline is oriented 80° from the North and is indicated by the vertical line on the left of the page.

66

ed in Fig. 6 as a function of the offshore distance. The weekly currents are nearly shore-parallel, in accord with observations (Blanton and Murthy 1975; Bull and Murthy 1980). Fig. 6 also shows frequent weekly current reversals and associated large lateral current shears in the mean flow. Blanton and Murthy (1975) report that high values of the lateral shear are associated with a general increase in all turbulent properties. Our results suggest that, despite large lateral current shears in the mean flow, the thermal bar tends to inhibit horizontal velocity fluctuations and cross-frontal turbulent momentum exchanges because the exchange coefficients and turbulence variables are much smaller in the spring than during summer stratified conditions as shown in the next sections.

Fig. 7 shows plots of the components of kinetic energy as a function of the offshore distance. Plate A represents summer and early fall conditions when the bar is no longer present (May 25 to October 23, 1990) and Plate B represents early spring conditions during the thermal bar episode (April 17 to May 24, 1990). Plate A is in agreement with typical post-bar conditions (Murthy and Dunbar 1981) where the turbulent kinetic energy q increases with the offshore distance, as inertial oscillations become predominant offshore. In the spring, the total kinetic energy E and mean kinetic energy e, increase to a peak located 3.24 kilometers offshore then decrease rapidly with the offshore distance. The turbulent kinetic energy q remains independent of the offshore distance (*i.e.*, depth) and contributes less than 6% to the total kinetic energy E while more than 94% of the total kinetic energy in the flow is attributable to the mean flow. Hence, free surface seiches, tidal oscillations, inertial motions, and all other small scale fluctuations account for a negligible fraction (less than 6%) of the total kinetic energy in the coastal margin during the thermal bar. These results suggest that when the thermal bar is present, horizontal turbulent motions are damped and have very little effect on the mean flow.

As stated earlier, exact values of horizontal exchange coefficients are not significant in themselves. These values serve as an indicator of dispersal tendencies in the flow and are presented in Fig. 8. Plate A represents synoptic conditions when the bar is no longer present (May 25 to October 23, 1990) and Plate B represents spring conditions, during the thermal bar episode (April 17 to May 24, 1990). In the post-bar case (A), the exchange coefficients increase with the offshore distance and remain homogeneous, $K = K_x \approx K_y$. Plate B shows that during the thermal bar, the longshore coefficients K_x decrease with the offshore distance. In addition, the horizontal exchange coefficients K_y are consistently smaller than K_x. These results lead us to argue that during the bar episode, momentum transfers occur predominantly along the bar and that cross-frontal transfers are relatively weak.

Fig. 8 also reveals that the cross-shore coefficients K_y remain relatively constant throughout the coastal margin and almost one order of magnitude smaller than the longshore counterparts during the thermal bar episode. This suggests that the main forcing function for K_y is not the bottom bathymetry nor the surface fluxes but the thermal bar.
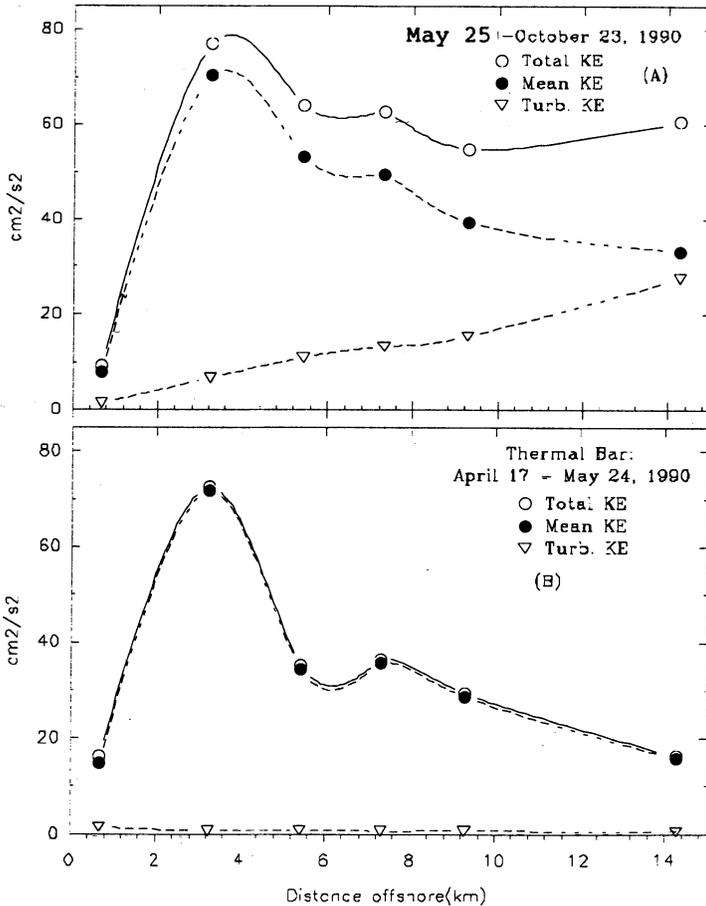
Fig. 7. Kinetic energy distribution during the thermal bar episode. Plate A represents late spring conditions when the bar is no longer present (May 25 to October 23,1990). Plate B represents spring values during the thermal bar episode (April 17 to May 24, 1990).

The horizontal exchange coefficients presented in Fig. 8 (Plate B) average $0.1 m^2/s$ and are several orders of magnitude smaller than typical coastal or oceanic values in the absence of the bar. Hence, it can be said that the thermal bar severely curtails dispersion tendencies, and particularly cross-frontal dispersion. Okubo (1968) argues that large lateral shears favor horizontal dispersion and large scale meandering in the flow. Low values of the horizontal exchange coefficients found here indicate a suppression of dispersion tendencies and support the damping effect of the thermal bar on cross-shore exchanges. During the thermal bar, the conventional assumption $K = K_x \approx K_y$ no longer holds and should be replaced by $K_y \approx c < K_x$ where c is a positive constant and K_x decreases with the offshore distance.
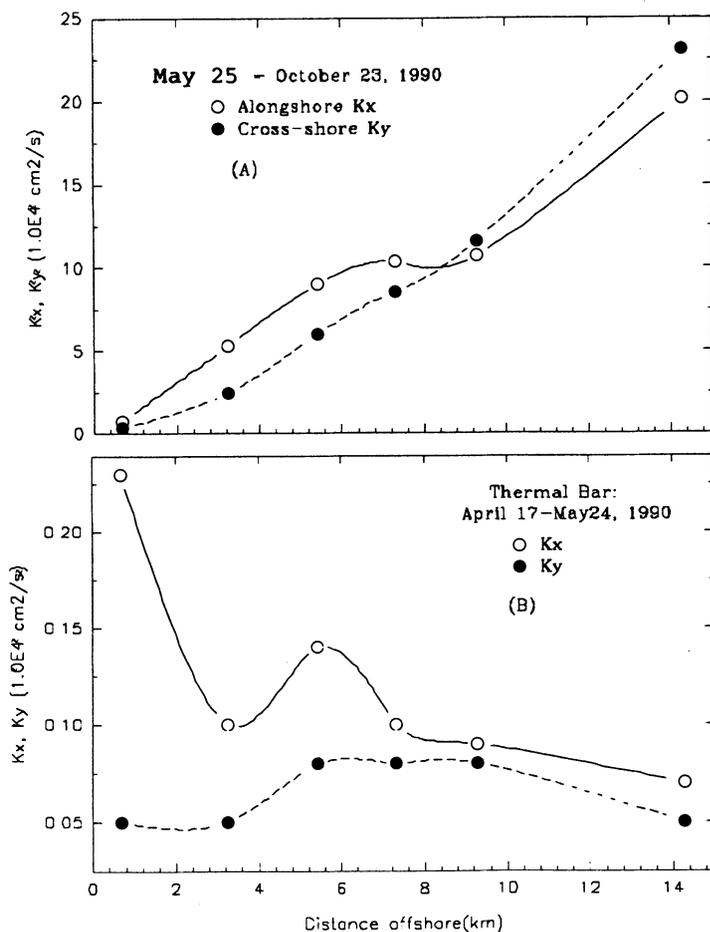
68

Fig. 8. Horizontal exchange coefficients (○ for K_x and ● for K_y) as a function of the offshore distance. Plate A represents values from late spring to fall when the bar is no longer present (May 25 to October 23,1990). Plate B represents spring values during the thermal bar episode (April 17 to May 24, 1990).

We note that the bar is a relatively small and dynamic region whereas the instrument array is static. Hence, the exchange coefficients at a given station represent temporal averages over the length of the record which encompasses the time period before, during, and after the bar has reached the given instrument. Despite this, the inhibiting effect of the bar on horizontal turbulent exchanges is clearly seen in Figs. 7 and 8. A more effective method of obtaining horizontal exchange coefficients exclusively associated with the bar would be to examine time series flow data from the immediate bar zone. However, this is a somewhat experimentally difficult task since the bar is dynamic.

69

Messon B. Gbah and Raj C. Murthy

Summary

Analysis of Eulerian time series flow data obtained from an array of moored buoys reveals the flow regime and cross-margin exchange characteristics in a nearshore zone of Lake Ontario during the thermal bar of April 17 to May 24, 1990. The theoretical backgrounds used to quantify horizontal exchange characteristics are derived from Hay and Pasquill (1959).

In the spring when the bar is present, the total kinetic energy E generally peaks close to the shore (3.24 kilometers offshore) then decreases rapidly outward. The turbulent kinetic energy appears depth-independent and represents less than 6% of the total kinetic energy in the flow. This suggests a strong damping of inertial oscillations and other small scale motions during the thermal bar episode. Moreover, horizontal exchange coefficients are several orders of magnitude smaller than synoptic oceanic and coastal values in the absence of the bar.

Sharp temperature gradients and lateral velocity shears characterize the bar. Okubo (1968) argues that large lateral shears favor horizontal dispersion and large scale meandering in the flow while Blanton and Murthy (1975) report that high values of the lateral shear are associated with a general increase in all turbulent properties. Despite the large velocity shears observed in the mean flow, cross-shore exchanges of turbulent momentum are severely inhibited and small scale horizontal fluctuations significantly damped during the thermal bar period.

Acknowledgments

References

Blanton, J. O. (1975) Nearshore lake currents measured during upwelling and downwelling of the thermocline in Lake Ontario, *J. Phys. Oceanogr., Vol.* 5, pp. 111-124.

Blanton, J. O., and Murthy, C. R. (1974) Observation of the lateral shear in the nearshore zone of a Great Lake, *J. Phys. Oceanogr., Vol.* 4 (4), pp. 660-663.

Brand, Stephen B. (1993) The effect of Thermal fronts on Fish Growth: A Bioenergetics Evaluation of Food and Temperature, *Estuaries, Vol.* 16 (1) pp.142-159.

Csanady, G. T. (1972a) The Coastal boundary layer in Lake Ontario, 1, The spring regime, *J. Phys. Oceanogr., Vol.* 2, pp. 41-53.

Csanady, G. T. (1972b) The Coastal boundary layer in Lake Ontario, 2, The summer-fall regime, *J. Phys. Oceanogr., Vol.* 2, pp. 168-176.

Franks, Peter J. (1992) Phytoplankton Blooms at Fronts: Patterns, Scales, and Physical Forcing Mechanisms, *Reviews in Aquatic Sciences, Vol.* 6 (2), pp. 121-137.

Gbah, Messon B. (1994) A Model of the Thermal Bar Based on a Second Order Turbulence Closure Scheme, Ph.D. Thesis, University of Michigan, Ann Arbor.

Graham, R. J. (1963) *Determination and analysis of a numerical smoothing weights,* NASA TR R-179, Marshall Space Flight Center, 28pp.

Haugen, D. A. (1966) Some Lagrangian properties of turbulence deduced from atmospheric diffusion experiments, *J. Appl. Meteor., Vol.* 5, pp. 646.

Hay, J. S., and Pasquill, F. (1959) Diffusion from a continuous source in relation to the spectrum and scale of turbulence, *Advances in Geophysics, Vol.* 6, Academic press, New York, pp. 345-365.

LeFevre, J. (1986) Aspects of the Biology of Frontal Systems, *Advances in Marine Biology, Vol.* 23, pp.163-299.

Lumley, L., and Danofsky, H. A. (1964) *The structure of atmospheric turbulence,* Interscience Publ., New York, London, Sydney.

Malm J., Mironov, D., Terzhevik, A., and Jönsson, L. (1994) Investigation of the Spring Thermal Regime in Lake Ladoga Using Filed and Satellite Data, *Limnology and Oceanography, Vol.* 39 (6), pp. 1333-1348.

Moll, R. A., Bratkovich, A., Chang, W. Y. B., and Pu, P., (1993) Physical, Chemical, and Biological Conditions Associated with the Early Stages of the Lake Michigan Vernal Thermal Front, *Estuaries, Vol.* 16 (1), pp. 92-103.

Murthy, C. R. and Blanton, J. O. (1975) Coastal zone climatological studies of the Laurentian reat Lakes, Proc. Second IWRA World Congress, Vol. V, pp. 431-448.

Murthy, C. R. and Dunbar, D. S., (1981) Structure of the Flow within the Coastal Boundary Layer of the Great Lakes, *J. Phys. Oceanogr., Vol.* 11 (11), pp. 1567-1577.

Okubo, A. (1968) Some remarks on the importance of the shear effect on horizontal diffusion, *Journal of Oceanographical Society of Japan, Vol.* 24 (2) pp. 6-69.

Rodgers, G. K. (1966) *The Thermal Bar in Lake Ontario, Spring 1965 and Winter 1965-66.* Pub. No. 15, Great Lakes Res. Division, The University of Michigan, Ann Arbor, pp. 369-374.

Schott, F., and Quadfasel, D. (1979) Lagrangian and Eulerian measurements of horizontal mixing in the Baltic. *Tellus, Vol.* 31, pp. 138-144.

Taylor, G. I. (1921) Diffusion by continuous movements, Proc. London Math. Soc., Vol. 20 (2), pp. 196-212.

Tikhomirov, A. I. (1963) The Thermal Bar of Lake Ladoga, Bull. (Izvestia) *All-Union Geogr. Soc. Vol., 95,* pp. 134-142, American Geophysical Union Trans., Soviet Hydro., Selected Paper No.2.

Tikhomirov, A. I. (1968) Temperature and Heat Contents of Lake Ladoga; In: *Thermal Regime Of Lake Ladoga,* S. V. Kalesnik (ed.), Leningrad University press, Leningrad, pp. 144-217.

Ziltinkevich, S. S., Kreiman, K. D., and Terzhevik, A. Y. (1992) The thermal bar, *J. Fluid Mechanics, Vol. 236,* pp. 27-42.

Address:
Messon B. Gbah,
The University of Michigan,
Naval Architecture and Marine Engineering,
2600 Draper Road,
Ann Arbor, Mi 48109-2145,
U.S.A.
Email: gbah@engin.umich.edu.

Raj C. Murthy,
National Water Research Institute,
867 Lakeshore Road,
P. O. Box 5050,
Burlington, Ont. L7R 4A6,
Canada.
Email: raj.murthy@cciw.ca

72